Acta Cryst. (1988). A44, 789-798

Symmetries and Beam Reduction in the Matrix Formulation of the Dynamical Theory of Fast Electrons

BY DENIS GRATIAS, MARIANNE CORNIER AND RICHARD PORTIER

Centre d'Etudes de Chimie Métallurgique/Centre National de la Recherche Scientifique, 15, rue Georges Urbain, 94407 Vitry, France

(*Received* 11 *December* 1987; *accepted* 5 *April* 1988)

Abstract

A survey of the symmetries of the two-dimensional scattering Hamiltonian of fast electrons is presented in order to minimize the size of the effective diffraction matrix. The principle of the method is to decompose the initial Hilbert space into the irreducible invariant subspaces corresponding to the different irreducible representations of the symmetry group of the Hamiltonian and to perform the diagonalization only into those subspaces which share common representations with the initial state. Both unitary and anti-unitary operators are considered. The analysis is based on space-group representations and applies for both symmorphic and non-symmorphic space groups.

Introduction

The dynamical theories for high-energy electron diffraction are essentially based on two complementary approaches: the quantum-mechanical matrix formulation (Sturkey, 1957, 1962; Tournarie, 1960; Howie & Whelan, 1961; Kambe, 1967) and the diffraction optics derivation (Cowley & Moodie, 1957; Cowley, 1975). Both theories are physically equivalent (Goodman & Moodie, 1974; Van Dyck, 1980); the first has been mostly developed for conventional electron microscopy whereas the second is essentially used for high-resolution calculations with the so-called multi-slice technique (Goodman & Moodie, 1974). A main advantage of the multi-slice technique is that it obviates the time- and space-consuming diagonalization of the diffraction matrix used in the quantum-mechanical approach by an iterative slice-to-slice calculation. Propagation and diffraction are treated separately, the first in reciprocal space and the second in real space. A disadvantage is that the accuracy of the method may decrease with increasing sample thickness whereas the diagonalization technique does not diverge, whatever the thickness of the sample. The multi-slice technique requires the extensive use of the fast Fourier transform algorithm for switching from reciprocal to direct space and *vice versa* at each step, which needs a large number of Fourier coefficients in order to remain accurate enough after many iterations. The essence of the matrix formulation is to make the optimum change of basis at once, *i.e.* to formulate the propagation of electrons in the solid on the natural eigenbasis of the Hamiltonian instead of switching from real to reciprocal space at each slice. Therefore, the number of beams introduced in the matrix method does not play the same role as in the multi-slice method and can be of a smaller size: it represents the dimension of the subspace of the Hilbert space upon which the minimization process of the diffracting Hamiltonian is performed. Once the lowest few eigenvectors of the Hamiltonian are sufficiently well approximated in this subspace, the calculation is as accurate as it is for a far larger number of 'beams' in the multi-slice method. But probably a substantial interest of the quantum-mechanical method is that it provides an elegant and clear formalism for the basic understanding of dynamical diffraction and allows for many versatile formal developments in a simple manner.

The purpose of the present paper is to give an extended description of the use of the symmetry properties of the diffraction process in the quantum-mechanical technique and to show how they may considerably simplify the dynamical calculations for high symmetry orientations.

The paper is divided as follows: in the first section, the general properties of symmetry of the scattering Hamiltonian are discussed. The rest of the paper is devoted to some explicit applications of the symmetry reduction technique with special attention to the case of non-symmorphic space groups and convergent-beam analyses.

I. Dynamical scattering Hamiltonian

The scattering of fast electrons by solids can be approximated by a two-dimensional (2D) pseudo-Hamiltonian, H, where the propagation direction is analogous to the time parameter in usual time-dependent quantum theory (Berry, 1971; Van Dyck, 1980; Gratias & Portier, 1983):

$$2K_z H = \sum_{\mathbf{q}} |\mathbf{q}\rangle(q^2 - \chi^2)\langle\mathbf{q}| + \sum_{(\mathbf{q},\mathbf{q}')} |\mathbf{q}'\rangle\langle\mathbf{q}'|\mathcal{V}(\boldsymbol{\rho}, z)|\mathbf{q}\rangle\langle\mathbf{q}|, \quad (1)$$

0108-7673/88/060789-10$03.00

where χ is the reciprocal vector from the projection of the centre of the Ewald sphere to the origin of the reciprocal lattice, K_z the z component of the incident-beam wave vector and $\mathbf{q}$ the set of 2D momentum transfer vectors (Fig. 1):

$$\mathbf{q} = \chi + \mathbf{G} \tag{2}$$

where $\mathbf{G}$ is a reciprocal-lattice vector. $\mathcal{V}(\boldsymbol{\rho}, z)$ is the scattering potential and $\langle \mathbf{q}'|\mathcal{V}(\boldsymbol{\rho}, z)|\mathbf{q}\rangle$ its 2D Fourier transform normalized by the 2D unit volume ω:

$$\langle \mathbf{q}'|\mathcal{V}(\boldsymbol{\rho}, z)|\mathbf{q}\rangle = (1/\omega)\int_{\omega} \mathcal{V}(\boldsymbol{\rho}, z) \times \exp[2i\pi(\mathbf{q}-\mathbf{q}')\cdot\boldsymbol{\rho}]\,\mathrm{d}^2\rho. \tag{3}$$

It is easily shown from (1) that the propagation term is diagonal on the reciprocal-space basis (set of plane waves), whereas the diffraction term $\mathcal{V}(\boldsymbol{\rho}, z)$ is diagonal on the real-space basis (set of Dirac masses).

A common further approximation consists of replacing the z-dependent potential by an average potential along the z propagation direction. This approximation has been shown to be valid for rapidly oscillating potentials along the z direction. Designating the resulting Fourier component by $V_{q,q'}$ and the thickness of the sample by t, so that

$$V_{q,q'} = t^{-1}\int_0^t \langle \mathbf{q}'|\mathcal{V}(\boldsymbol{\rho}, z)|\mathbf{q}\rangle\,\mathrm{d}z, \tag{4}$$

we obtain a reduced normalized z independent Hamiltonian $\mathcal{H}$ where the eigenvalues are now shifted relative to the constant χ^2 obliquity factor:

$$\mathcal{H} = \sum_{\mathbf{q}} |\mathbf{q}\rangle q^2 \langle \mathbf{q}| + \sum_{(\mathbf{q},\mathbf{q}')} |\mathbf{q}\rangle V_{q,q'}\langle \mathbf{q}'|. \tag{5}$$

The diagonal term (self excitation) increases quadratically with $|\mathbf{q}|$ whereas the off-diagonal terms decrease to zero for large $|\mathbf{q}|$ values; for reciprocal nodes far away from the Ewald sphere, the Hamiltonian is almost diagonal in such a manner that there will be no noticeable transition between such states and the initial one $|\chi\rangle$. It is therefore possible to limit the $\{|\mathbf{q}\rangle\}$ basis to those kets whose self excitation is not too large compared with the upper value of the $|V_{q,q'}|$'s.

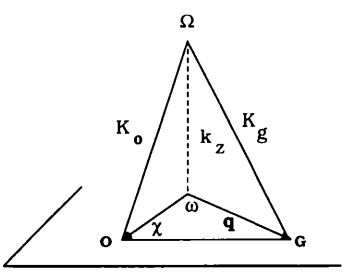

Fig. 1. Definition of the dynamical parameters; $\mathbf{K}_0$ is the incident wave vector, ω is the projection of the centre of the Ewald sphere onto the diffracting plane and χ is the obliquity vector $\boldsymbol{\omega}\mathbf{O}$ where O is the origin of the reciprocal space. A diffracting vector is defined by $\mathbf{q} = \chi + \mathbf{G}$ where $\mathbf{G}$ is a reciprocal-lattice vector.

The scattering Hamiltonian is a 2D version of the familiar one-electron Hamiltonian. As a consequence of that, the diagonalization can always be performed for initial states $|\chi\rangle$ with wave vectors lying within the first Brillouin zone. For instance, the simulation of a tilted dark-field image requires no additional calculations once the diagonalization has been achieved in bright field. The tilting consists essentially of a relabelling of the incident and diffracted beams.

The diffracted beams and images are obtained after standard diagonalization techniques. If $|j\rangle$ and γ_j are the eigenvectors and eigenvalues of (5), the evolution operator $\mathcal{U}(z)$ at thickness z is written as

$$\mathcal{U}(z) = \sum_{\mathbf{j}} |\mathbf{j}\rangle \exp(i\pi\gamma_j z)\langle \mathbf{j}|, \tag{6a}$$

leading to the expressions of the diffracted beams $\Phi_{\mathbf{q}}(z)$ and images $\mathcal{I}(\boldsymbol{\rho}, z)$:

$$\Phi_{\mathbf{q}}(z) = \langle \mathbf{q}|\mathcal{U}(z)|\chi\rangle = \sum_{\mathbf{j}} \langle \mathbf{q}|\mathbf{j}\rangle \exp(i\pi\gamma_j z)\langle \mathbf{j}|\chi\rangle \tag{6b}$$

$$\mathcal{I}(\boldsymbol{\rho}, z) = \left|\sum_{(\mathbf{q},\mathbf{q}')} \langle \boldsymbol{\rho}|\mathbf{q}'\rangle \exp[-i\Phi(\mathbf{q}', \mathbf{q})]\langle \mathbf{q}|\mathcal{U}(z)|\chi\rangle\right|^2, \tag{6c}$$

where $\Phi(\mathbf{q}, \mathbf{q}')$ represents the phase of the aberration function.

A similar derivation can be carried out for quasicrystals with the only difference that the set of $\mathbf{q}$ vectors to be considered is a $\mathbb{Z}$ modulus* instead of being on a 2D lattice (Cornier, Portier & Gratias, 1986). In any case, each individual $\mathbf{q}$ vector is uniquely labelled by a set of N integer indices ($N = 3$ for crystals, $N = 3 + d$ for d-dimensional modulated structures and $N > 3$ for quasicrystals). A common feature of presently recognized topologically long-range ordered structures is the fact that the observable reflections are located at finite distances from each other, leading to a discrete aspect of the diffraction pattern, even if the geometric measure of the Fourier transform is mathematically dense. One of the major problems in simulating this kind of structure with the multi-slice technique is the absence of periodicity in physical space which makes the use of fast Fourier transforms impossible without introducing an artificial periodicity. In the quantum-mechanical approach, the only problem is the criterion of selecting, among a dense set, only those beams which actually are predominant in the diffraction. It turns out that a substantial number of beams is required for avoiding numerical instabilities in the diagonaliz-

* A $\mathbb{Z}$ modulus is a vector space built on a ring; in the present case, the ring is the set of the natural integers and the $\mathbb{Z}$ modulus is isomorphic to a lattice in a space of dimension equal to the rank of the $\mathbb{Z}$ modulus.

ation process. For example, an exact fivefold orientation of an icosahedral quasicrystal shows a diffraction pattern with more than 500 excited beams. An artificial truncation in the number of beams may lead to important variations in the eigenvalues and eigenvectors of the scattering Hamiltonian. In such cases of high-symmetry patterns, the beam reduction technique is the most efficient: the original 561 beams reduce to a final dynamical matrix with only 37 orbits (Cornier *et al.*, in preparation).

II. Symmetries and beam reductions

The calculation of the evolution operator (6*a*) is largely simplified by introducing the symmetry operations of the system which lead to a primary block diagonalization. The physical guideline of the beam reduction technique is the following: the dynamical theory consists in calculating the transition probabilities between the initial state $|\chi\rangle$ and a given chosen state $|\mathbf{q}\rangle$; this probability has to satisfy two basic conditions if it is not to be trivially zero:

(i) there must exist eigenvectors of (5) with the same symmetry as $|\chi\rangle$;

(ii) among these states, only those also having the same symmetry as $|\mathbf{q}\rangle$ have to be considered; for instance if $|\chi\rangle$ and $|\mathbf{q}\rangle$ belong to two orthogonal symmetry states, the transition probability is zero.

Hence, the sole eigenstates required for the diffraction calculation are those which transform according to the irreducible representations of the symmetry group of the Hamiltonian which are common to both the initial and the final states.

Such beam reductions were proposed several years ago for specific cases (Blume, 1966; Fukuhara, 1966; Fisher, 1968; Tinnappel & Kambe, 1975; Kogiso & Takahashi, 1977; Vergasov, Chukhovskii & Pinsker, 1982) and a systematic procedure based on space-group symmetry has recently been published (Takeda, 1986, 1987) in the framework of the Howie & Whelan (1961) formulation. Our main purpose in the present paper is to give an explicit derivation consistent with the quantum-mechanical formalism in including both the unitary and anti-unitary symmetries of the system. The key point of our technique consists of expressing all operators directly in the Hilbert space which reduces the handling of group representation theory to elementary algebraic calculations.

Also of primary importance in the recent development of the convergent-beam technique is the recognition of actual symmetries of the observed 3D structure from 2D diffraction patterns. Discussions on the symmetry of the convergent-beam patterns are numerous and well documented, especially with the publication of the impressive paper by Buxton, Eades, Steeds & Rackham (1976) (see also Eades, 1980). We will discuss here some of these previous results in the framework of group theory as developed by Wigner (1932) for general anti-unitary operators and show how it unites the different approaches to this subject. Special attention will be given to the case of non-symmorphic space groups in the totally symmetrical Laue position.

II.1. *2D invariance space group of the Hamiltonian*

The 2D invariance space group of the Hamiltonian is the 2D space group of the projected structure for any value of χ. For a general χ, the application of the symmetry elements of the projected structure generally transforms a $\mathbf{q}$ vector of the reciprocal lattice into a vector which does not belong to the same reciprocal lattice (remember that $\mathbf{q}$ is a diffraction vector originating from the projection of the Ewald sphere and not from the origin of the reciprocal lattice). The number η of different reciprocal lattices induced by the symmetry group of the projected potential is obtained in the following way: let $\mathcal{G}$ be the centred holohedral group of the reciprocal 2D lattice and let $\mathcal{G}_\chi$ be the little group of χ defined by

$$\mathcal{G}_\chi = \{g \in \mathcal{G}, g\boldsymbol{\chi} = \boldsymbol{\chi} + \mathbf{G}\}. \tag{7}$$

The number η of independent reciprocal lattices is the index of $\mathcal{G}_\chi$ onto $\mathcal{G}$:

$$\eta = \text{index}(\mathcal{G}_\chi / \mathcal{G}). \tag{8}$$

Of course, only the reciprocal lattice generated by the χ vector is excited in practice and the effective space group is $\mathcal{G}_\chi$. However, we will see that considering the fully symmetric basis (set of all reciprocal lattices deduced by the symmetry of the projected potential) helps in understanding the hidden symmetries of the Hamiltonian in the general case.

II.2. *Symmetry operations in Hilbert space; eigenvectors and eigenvalues*

There are two basic types of symmetry operations: those which transform the propagation direction into itself and those which invert it; Although they all are essentially the geometric unitary operations induced by the 3D symmetries of the solid, the latter are equivalent to the products of 2D symmetry operations by the time-reversal anti-unitary operator $\mathcal{K}$ (see Messiah, 1965).

In the bracket notation, a 2D symmetry operation $(\alpha|\mathbf{t})$ acting as $(\alpha|\mathbf{t})\boldsymbol{\rho} = \alpha\boldsymbol{\rho} + \mathbf{t}$ in direct space (Seitz, 1936) can be written in Hilbert space as

$$(\alpha|\mathbf{t}) = \sum_{\mathbf{q}} |\alpha^{-1}\mathbf{q}\rangle \exp(2i\pi\mathbf{q}\mathbf{t})\langle\mathbf{q}|. \tag{9}$$

Such unitary operators correspond to the 3D symmetry operations which preserve the z direction. They have a matrix representation which consists of an infinite set of diagonal blocks, each block containing the star of the $\mathbf{q}$ vector considered. A special case of those operators is the translation operators, $(1|\mathbf{T})$,

which are diagonal on the Hilbert $\{|\mathbf{q}\rangle\}$ basis with eigenvalues $\exp(2i\pi\mathbf{qT})$,

$$(1|\mathbf{T}) = \sum_{\mathbf{q}} |\mathbf{q}\rangle \exp(2i\pi\mathbf{qT})\langle\mathbf{q}|. \tag{10}$$

The basic anti-unitary transformation $\mathcal{K}$ [defined as 1_R in Buxton *et al.*'s (1976) notation] is defined by

$$\langle\mathbf{v}|(\mathcal{K}|\mathbf{u}\rangle) = \sum_{\mathbf{q}} \langle\mathbf{v}|-\mathbf{q}\rangle\langle\mathbf{q}|\mathbf{u}\rangle^* \tag{11a}$$

$$(\langle\mathbf{v}|\mathcal{K})|\mathbf{u}\rangle = \sum_{\mathbf{q}} \langle\mathbf{v}|-\mathbf{q}\rangle^*\langle\mathbf{q}|\mathbf{u}\rangle. \tag{11b}$$

Multiplication of this anti-unitary operator by any of the former unitary operations leads to the other basic '*R*-type' operations, say $\mathcal{K}'$:

$$(\mathcal{K}'|\mathbf{u}\rangle) = \sum_{\mathbf{q}} |-\mathbf{q}\rangle\langle\mathbf{q}|\mathbf{u}\rangle^* = (2_R|\mathbf{u}\rangle^*) \tag{12a}$$

$$(\mathcal{K}'(2|0)|\mathbf{u}\rangle) = \sum_{\mathbf{q}} |-2\mathbf{q}\rangle\langle\mathbf{q}|\mathbf{u}\rangle^*$$

$$= \sum_{\mathbf{q}} |\mathbf{q}\rangle\langle\mathbf{q}|\mathbf{u}\rangle^* = (1_R|\mathbf{u}\rangle^*) \tag{12b}$$

$$(\mathcal{K}'(m|\mathbf{t})|\mathbf{u}\rangle) = \sum_{\mathbf{q}} |-m\mathbf{q}\rangle \exp(-2i\pi\mathbf{q}.\mathbf{t})\langle\mathbf{q}|\mathbf{u}\rangle^*$$

$$= (m_R|\mathbf{u}\rangle^*). \tag{12c}$$

The cornerstone of the beam reduction technique is a change of the $\{|\mathbf{q}\rangle\}$ basis of the Hilbert space into a symmetry-adapted basis constructed with the eigenvectors of these symmetry operations and selection of the irreducible subspaces that transform according to the initial $|\chi\rangle$ state.

The rotations in 2D space are always reducible [an origin can be chosen for the rotation operator to be written as $(\alpha|\mathbf{0})$]. The set of the corresponding eigenvectors ω^k and eigenvectors $|\mathbf{Q}_\alpha^{(k)}\rangle$ are, for each $n \times n$ block,

$$|\mathbf{Q}_\alpha^{(k)}\rangle = \frac{1}{\sqrt{n}} \sum_{j=0}^{n-1} \omega^{jk} |\mathbf{q}_k\rangle, \tag{13}$$

where n is the order of the rotation, $\omega = e^{2i\pi/n}$ and $\mathbf{q}_k$ are the vectors of the $\mathbf{q}$ star induced by the rotation considered.

Mirrors $(m|\mathbf{t})$ can be pure $(\mathbf{t} = \mathbf{T})$ or glide $(\mathbf{t} = \mathbf{T}/2)$ (the four non-symmorphic 2D space groups are *pg*, *pmg*, *pgg* and *p4g*). Their eigenvectors and eigenvalues are, for each $(\mathbf{q}, m\mathbf{q})$ 2×2 block,

$$|\mathbf{Q}_g^{(1)}\rangle = \frac{1}{\sqrt{2}}\{|\mathbf{q}\rangle + \exp[i\pi(\mathbf{q}-m\mathbf{q})\mathbf{t}]|m\mathbf{q}\rangle\}$$

$$\lambda_1 = \exp[i\pi(\mathbf{q}+m\mathbf{q})\mathbf{t}] \tag{14a}$$

$$|\mathbf{Q}_g^{(2)}\rangle = \frac{1}{\sqrt{2}}\{|\mathbf{q}\rangle - \exp[i\pi(\mathbf{q}-m\mathbf{q})\mathbf{t}]|m\mathbf{q}\rangle\}$$

$$\lambda_2 = -\lambda_1. \tag{14b}$$

Finally, it is easily shown that for each pair $(q, -q)$, the orthogonal vectors $|\mathbf{u}_q\rangle$ and $|\mathbf{v}_q\rangle$ defined by

$$|\mathbf{u}_q\rangle = \frac{1}{\sqrt{2}}(|\mathbf{q}\rangle + |-\mathbf{q}\rangle); \qquad |\mathbf{v}_q\rangle = \frac{i}{\sqrt{2}}(|\mathbf{q}\rangle - |-\mathbf{q}\rangle) \tag{15}$$

are eigenvectors of the basic anti-unitary operation $\mathcal{K}$.

III. Beam reduction from anti-unitary operations

III.1. *Real Hamiltonian and real basis*

In the absence of a phenomenological absorption term, the $\mathcal{K}$ operator commutes with the Hamiltonian ($\mathcal{H}$ is a real operator) and therefore a basis can always be found for which the coefficients of the Hamiltonian are real numbers. This basis is defined by the eigenvectors $|\mathbf{u}\rangle$ and $|\mathbf{v}\rangle$ of $\mathcal{K}$ which are the adequate real basis for the Hamiltonian of non-centrosymmetric structures (for the centrosymmetric case, the Hamiltonian basis is real *ab initio*). The explicit calculation of the matrix elements of the Hamiltonian gives

$$\begin{aligned}
\langle\mathbf{u}_{q'}|\mathcal{H}|\mathbf{u}_q\rangle &= q^2\delta_{q,q'} + |V_{q',q}|\cos\varphi_{q',q} + |V_{q',-q}|\cos\varphi_{q',-q} \\
\langle\mathbf{v}_{q'}|\mathcal{H}|\mathbf{v}_q\rangle &= q^2\delta_{q,q'} + |V_{q',q}|\cos\varphi_{q',q} \\
&\quad - |V_{q',-q}|\cos\varphi_{q',-q} \\
\langle\mathbf{u}_{q'}|\mathcal{H}|\mathbf{v}_q\rangle &= -|V_{q',q}|\sin\varphi_{q',q} - |V_{-q',q}|\sin\varphi_{-q',q} \\
\langle\mathbf{v}_{q'}|\mathcal{H}|\mathbf{u}_q\rangle &= |V_{q',q}|\sin\varphi_{q',q} + |V_{q',-q}|\sin\varphi_{q',-q}
\end{aligned} \tag{16}$$

where $V_{q',q} = |V_{q',q}|\exp(i\varphi_{q',q})$.

Of course, the initial state $|\chi\rangle$ has now to be written as

$$|\chi\rangle = \frac{1}{\sqrt{2}}(|\mathbf{u}_\chi\rangle - i|\mathbf{v}_\chi\rangle)$$

$$= \left(\frac{1}{\sqrt{2}}, 0, 0, \ldots, \frac{-i}{\sqrt{2}}, 0, 0, \ldots, 0\right). \tag{17}$$

Two cases have to be considered (Fig. 2): if the initial obliquity vector $\boldsymbol{\chi}$ is such that $2\boldsymbol{\chi} = \mathbf{G}$, a vector of the reciprocal lattice, then $\mathbf{q}$ and $-\mathbf{q}$ belong to the same lattice and $V_{-q',q}$ is generally not zero, but the

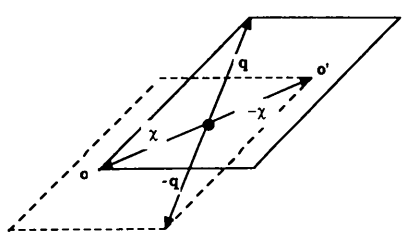

Fig. 2. For $\boldsymbol{\chi}$ in general position, it is useful to introduce the different virtual reciprocal lattices which restore the full symmetry of the projected potential; each time $\boldsymbol{\chi}$ is at a special position, these lattices superimpose on top of each other, leading to beam reduction.

number of rows and columns of the matrix is the same as the initial number of beams. The reduction has the effect of only transforming the Hermitian matrix into an equivalent $N \times N$ real symmetric matrix. This means that the Hamiltonian matrix is real for diffractions in which one at least of the diffracting beams is in the exact Bragg position, independent of the actual symmetry of the structure. If $\mathcal{G}_\chi$ contains either 2_R (centrosymmetric structures) or 1_R (projection of the Ewald sphere at some special positions) then the excited reciprocal-lattice vectors already form a real basis when properly coupled by the $|\mathbf{u}_q\rangle$ and $|\mathbf{v}_q\rangle$ eigenvectors defined by

$$|\mathbf{u}_q\rangle = \frac{1}{\sqrt{2}}[|\mathbf{q}\rangle + (\mathcal{K}'|\mathbf{q}\rangle)] \qquad (18a)$$

$$|\mathbf{v}_q\rangle = \frac{-i}{\sqrt{2}}[|\mathbf{q}\rangle - (\mathcal{K}'|\mathbf{q}\rangle)]. \qquad (18b)$$

If $\boldsymbol{\chi}$ is at a general location then the introduction of an additional reciprocal lattice centred at $-\boldsymbol{\chi}$ increases the number of rows and columns by a factor of two but again leads to a new $2N \times 2N$ real symmetric matrix. In this latter case, all terms of the kind $V_{q',-q}$ are zero in the set of expressions (16).

This simple analysis shows that for the very important case of the Laue symmetrical orientation ($\boldsymbol{\chi} = \mathbf{0}$) it is always possible to transform the scattering matrix into a real symmetrical one of the same size, whatever the symmetry of the structure. The expressions of the diffracted beams are

$$\Phi_{\mathbf{q}}(z) = \tfrac{1}{2}[\langle \mathbf{u}_q|\mathcal{U}(z)|\mathbf{u}_\chi\rangle + \langle \mathbf{v}_q|\mathcal{U}(z)|\mathbf{v}_\chi\rangle + i(\langle \mathbf{v}_q|\mathcal{U}(z)|\mathbf{u}_\chi\rangle - \langle \mathbf{u}_q|\mathcal{U}(z)|\mathbf{v}_\chi\rangle)]. \qquad (19)$$

III.2. *The 2_1-fold dynamical extinction (Gjønnes & Moodie, 1965)*

As quoted before, the general anti-unitary operations used in electron microscopy result in the product of the time-reversal operation $\mathcal{K}$ with any of the unitary operations. There are special interesting cases where the reciprocal lattice transforms into itself by a binary anti-unitary operator which is not $\mathcal{K}$ itself. Such is the case in the example seen in Fig. 3(*a*), where the projection of the Ewald sphere is located on the mid-perpendicular of a **G** reciprocal vector along a mirror direction defining the x axis; the anti-unitary invariance is due to the m_R operator and not to 1_R. The 'two-colour' 2D space group $\mathcal{C}_\chi$* is the union

$$\mathcal{C}_\chi = G_\chi \cup (m_R|\mathbf{t})G_\chi, \qquad (20)$$

where G_χ is a subgroup of the symmetry group of the projected potential, say $G_{\mathcal{K}}$, defined by

$$G_{\mathcal{K}} = \{(\alpha|\mathbf{t});\ V[(\alpha|\mathbf{t})\boldsymbol{\rho}] = V(\boldsymbol{\rho})\}, \qquad (21a)$$

such that

$$G_\chi = \{(\alpha|\mathbf{t}) \in \mathcal{G}_{\mathcal{K}};\ \alpha\boldsymbol{\chi} = \boldsymbol{\chi} + \mathbf{G}\}. \qquad (21b)$$

The coset $(m_R|\mathbf{t})G_\chi$ contains the anti-unitary operations

$$m_R\boldsymbol{\chi} = -\boldsymbol{\chi} + \mathbf{G}. \qquad (22)$$

The basic properties of this anti-unitary operator depend on the square of the operator (see Wigner, 1932),

$$(m_R|\mathbf{t})^2 = \sum_{\mathbf{q}} |\mathbf{q}\rangle \exp[2i\pi(m\mathbf{q} + \mathbf{q})\mathbf{t}]\langle \mathbf{q}|. \qquad (23)$$

First of all, the phases of the diagonal terms are equal: let **G** be the reciprocal-lattice vector associated with **q**, $\mathbf{q} = \boldsymbol{\chi} + \mathbf{G}$; $m\mathbf{G} + \mathbf{G}$ is along the x axis and has an even h index; the translation **t** is either a primitive translation (pure mirror) or $\mathbf{t} = \mathbf{T}/2$ (glide) in such a manner that for any **q** and any type of mirror, the scalar product $(m\mathbf{G} + \mathbf{G})\mathbf{t}$ is an integer. If the mirror is pure, the remaining term $\exp[2i\pi(m\boldsymbol{\chi} + \boldsymbol{\chi})\mathbf{t}]$ is equal to 1. For a glide, this term is either +1 if $\boldsymbol{\chi}$ is

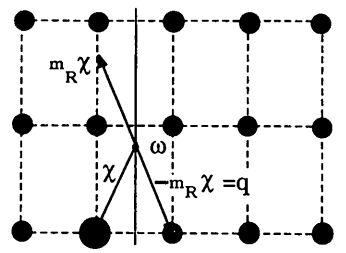

(*a*)

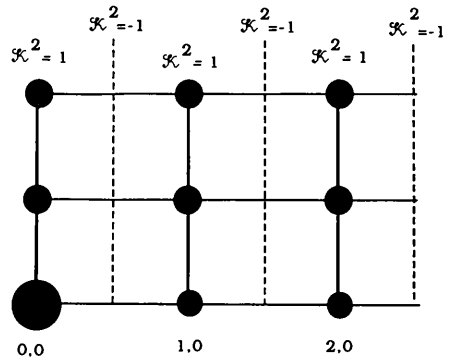

(*b*)

Fig. 3. (*a*) If $\boldsymbol{\chi}$ is on the mid-perpendicular of a diffracting vector with a *pg*, *pmg* or *p*4*g* 2D space group, the $-m_R\boldsymbol{\chi}$ lattice superimposes exactly with the original reciprocal lattice. (*b*) In that case, the effective anti-unitary operation $\mathcal{K}$ involved in the problem has a square operator equal to ± 1 according to the location of $\boldsymbol{\chi}$. If the square is equal to -1, then the **q** vector equal to $-m_R\boldsymbol{\chi}$ is dynamically absent.

* Actually the group would be better designated as a double group rather than a colour group since the coset contains anti-unitary operations.

Table 1. *Character table for the three possible restricted space groups (pm, pg and cm) of a diffracting vector*

$\Phi = 2\pi\boldsymbol{\chi}\cdot\mathbf{t}$

$G_\chi = pm$	$(1\|0, n_y)$	$(1\|1, n_y)$	$(1\|2, n_y)$	...	$(m_x\|0, n_y)$	$(m_x\|1, n_y)$	$(m_x\|2, n_y)$	...			
$\Gamma(\boldsymbol{\chi})$	1	$e^{i\Phi}$	$e^{2i\Phi}$	...	1	$e^{i\Phi}$	$e^{2i\Phi}$	...			
$G_\chi = pg$	$(1\|0, n_y)$	$(1\|1, n_y)$	$(1\|2, n_y)$	...	$(m_x\|\frac{1}{2}, n_y)$	$(m_x\|\frac{3}{2}, n_y)$	...				
$\Gamma(\boldsymbol{\chi})$	1	$e^{i\Phi}$	$e^{2i\Phi}$	...	$e^{i\Phi/2}$	$e^{i3\Phi/2}$	...				
$G_\chi = cm$	$(1\|0, n_y)$	$(1\|1, n_y)$	...	$(1\|\frac{1}{2}, n_y)$	$(1\|\frac{3}{2}, n_y)$	...	$(m_x\|0, n_y)$	$(m_x\|1, n_y)$	...	$(m_x\|\frac{1}{2}, n_y)$	$(m_x\|\frac{3}{2}, n_y)$	...
$\Gamma(\boldsymbol{\chi})$	1	$e^{i\Phi}$	...	$e^{i\Phi/2}$	$e^{i3\Phi/2}$	...	1	$e^{i\Phi}$	...	$e^{i\Phi/2}$	$e^{i3\Phi/2}$	...

on the mid-perpendicular of an even-h-index reflection, or -1 if it is on the mid-diagonal of an odd-h-index reflection (see Fig. 3*b*):

$$\mathcal{K}'^2 = \exp[2i\pi(m\boldsymbol{\chi}+\boldsymbol{\chi})\mathbf{t}] = \pm 1. \tag{24}$$

The case $\mathcal{K}'^2 = -1$ corresponds to a basic rule of dynamical absence: from a simple examination of the geometry of the diffraction pattern it is easily shown that the $\mathbf{q}$ vector defined by $\mathbf{q} = -m\boldsymbol{\chi}$ satisfies the relations

$$(\mathcal{K}|\mathbf{q}\rangle) = |-m\mathbf{q}\rangle \exp(-2i\pi\mathbf{q}\mathbf{t}) = |\boldsymbol{\chi}\rangle \exp(-2i\pi\mathbf{q}\mathbf{t}) \tag{25a}$$

$$(\langle\boldsymbol{\chi}|\mathcal{K}) = \exp(-2i\pi m\boldsymbol{\chi}\mathbf{t})\langle -m\boldsymbol{\chi}| = \exp(2i\pi\mathbf{q}\mathbf{t})\langle\mathbf{q}|, \tag{25b}$$

such that the diffracted amplitude can be written as

$$\langle\mathbf{q}|\mathcal{U}|\boldsymbol{\chi}\rangle = \sum_{\mathbf{j}}{}'\langle\mathbf{q}|\mathbf{j}\rangle \exp(i\pi\gamma_j z)\langle\mathbf{j}|\boldsymbol{\chi}\rangle + \langle\mathbf{q}|(\mathcal{K}|\mathbf{j}\rangle) \exp(i\pi\gamma_j z)(\langle\mathbf{j}|\mathcal{K}^\dagger)|\boldsymbol{\chi}\rangle \tag{26}$$

where the eigenstates $|\mathbf{j}\rangle$ have been recombined by pairs $|\mathbf{j}\rangle$ and $(\mathcal{K}|\mathbf{j}\rangle)$. After a few algebraic manipulations using the properties of $\mathcal{K}$ and the relations (25), we finally obtain

$$\langle\mathbf{q}|\mathcal{U}|\boldsymbol{\chi}\rangle = \sum_{\mathbf{j}}{}'\langle\mathbf{q}|\mathbf{j}\rangle \exp(i\pi\gamma_j z)\langle\mathbf{j}|\boldsymbol{\chi}\rangle - \langle\mathbf{q}|\mathbf{j}\rangle \exp(i\pi\gamma_j z)\langle\mathbf{j}|\boldsymbol{\chi}\rangle = 0, \tag{27}$$

which shows that, for this particular chosen $\mathbf{q}$ vector and this orientation, the diffracted intensity is zero for a glide mirror: this is the well known 2_1-fold extinction first demonstrated in a famous paper by Gjønnes & Moodie (1965) (geometrical locus noted *B* in their original paper). Interestingly enough, we notice here that this extinction is due to anti-unitary symmetry with the consequence that this extinction should appear only for the elastic part of the diffraction spectrum.

IV. Beam reduction from unitary operations

Most of the efficiency of the beam reduction technique arises from the unitary operations for high-symmetry orientations of the incident beam. From now on, we shall restrict our attention to the sole unitary coset G_χ of $\mathscr{C}_\chi$ as defined in (21).

Let us designate by restricted little group γ_χ the subgroup of G_χ defined by

$$\gamma_\chi = \{(\alpha|\mathbf{t}) \in G_\chi;\ \alpha\boldsymbol{\chi} = \boldsymbol{\chi}\}. \tag{28}$$

If $\boldsymbol{\chi}$ is along a special line (a mirror), say the x axis, passing through the origin, the only possible restricted groups are *pm*, *Cm* or *pg*. We can sort the symmetry elements of γ_χ by regrouping in the same class all the symmetry elements which differ only by the translation part such that the differences between any two translations satisfy $\boldsymbol{\chi}\cdot\mathbf{t} = n$. If $\boldsymbol{\chi}$ is generic, there will be an infinite discrete number of such classes. By contrast, if $\boldsymbol{\chi}$ projects at a rational position along x then the number of classes will be finite. In all cases, the ket $|\boldsymbol{\chi}\rangle$ defines an irreducible representation (because of dimension 1), say $\Gamma(\boldsymbol{\chi})$, of γ_χ. The character tables for *pm*, *pg* and *Cm* are given in Table 1. The same procedure can be applied starting from a ket $|\mathbf{q}\rangle$ associated with a $\mathbf{q}$ vector aligned along the x axis (and, therefore, with the same restricted little group). For *pm* and *Cm* groups, the two representations $\Gamma(\boldsymbol{\chi})$ and $\Gamma(\mathbf{q})$ are the same since $\mathbf{q}$ and $\boldsymbol{\chi}$ differ by a reciprocal-lattice translation and *pm* and *Cm* have only primitive translation operations. For the *pg* group, the 1/2 non-primitive translation along x generates two possible representations for $\Gamma(\mathbf{q})$ according to the parity of the index h of $\mathbf{q}$. Only one of those representations is identical to $\Gamma(\boldsymbol{\chi})$; the reflections with odd h index have a different representation from $\boldsymbol{\chi}$ and therefore zero transition probability; this is the first geometrical locus in the original Gjønnes & Moodie (1965) derivation (labelled locus *A* in their paper). Contrary to locus *B* seen in the preceding section, this extinction rule arises from unitary transformation and applies as well for elastic as for inelastic scattering.

V. Examples

V.1. *The fully symmetrical Laue case*

The most important case of non-trivial symmetry of the incident beam is the symmetrical Laue case defined by $\boldsymbol{\chi} = \mathbf{0}$. This case is of primary importance in high-resolution imaging and the beam reduction

technique is both efficient and especially simple to apply. This is actually the case which has been most studied with respect to the point-group symmetry. The present approach, including the translational symmetry, allows for the derivation of beam reduction in the case of non-symmorphic space groups.

The invariance space group of χ is obviously the invariance space group of the projected structure

$$\gamma_\chi = G_{\mathscr{H}}. \tag{29}$$

It is therefore sufficient to construct - if it exists - the totally symmetric linear combination associated with diffracting $\mathbf{q}$ star and to remove all the other possible combinations. The dimension of the pertinent scattering matrix is then equal to the number of excited orbits. This problem is simple for the case of symmorphic space groups but requires some additional considerations in the non-symmorphic case.

We first assume that the dynamically absent orbits (locus A due to glide mirrors) have been eliminated. Let $\gamma_\mathbf{q}$ be the restricted little group defined by (28) of a given allowed $\mathbf{q}$ vector; $\gamma_\mathbf{q}$ is a subgroup of γ_χ. The totally symmetric ket, say $|\mathbf{Q}_q\rangle$, is obtained by coset decomposition of γ_χ onto $\gamma_\mathbf{q}$:

$$\gamma_\chi = \bigcup_{k=1}^{n} (\alpha_k|\mathbf{t}_k)\gamma_\mathbf{q}, \tag{30}$$

where each coset transforms the arbitrary initial chosen representative, say $\mathbf{q}_0$, of the $\mathbf{q}$ star into its equivalents $\mathbf{q}_k$ and n is the index of γ_χ onto $\gamma_\mathbf{q}$. The representation of γ_χ on the $\mathbf{q}$ orbit is obtained by calculating the transforms of the ket $|\mathbf{q}_0\rangle$ by each of the n cosets:

$$(\alpha_k|\mathbf{t}_k)\gamma_\mathbf{q}|\mathbf{q}_0\rangle = \exp(2i\pi\mathbf{q}_0\cdot\mathbf{t}_k)|\alpha_k^{-1}\mathbf{q}_0\rangle. \tag{31}$$

The totally symmetric linear combination sought is therefore

$$|\mathbf{Q}_q\rangle = \frac{1}{\sqrt{n}}\sum_{k=1}^{n}\exp(2i\pi\mathbf{q}_0\cdot\mathbf{t}_k)|\mathbf{q}_k\rangle. \tag{32}$$

For symmorphic space groups, this relation leads to the well known totally symmetric sum, but gives non-trivial results when applied to the non-symmorphic space groups. The values of the phase coefficients $\eta_k = \exp(2i\pi\mathbf{q}_0\cdot\mathbf{t}_k)$ are given in Fig. 4 for the four cases of non-symmorphic 2D space groups.

The calculation of the Hamiltonian-reduced matrix is given by

$$\langle\mathbf{Q}_{q'}|\mathscr{H}|\mathbf{Q}_q\rangle = \frac{1}{\sqrt{n}}\frac{1}{\sqrt{n'}} \times \sum_{(k,k')}\exp[2i\pi(\mathbf{q}_0\cdot\mathbf{t}_k - \mathbf{q}'_0\cdot\mathbf{t}'_{k'})]\langle\mathbf{q}'|\mathscr{H}|\mathbf{q}\rangle, \tag{33}$$

as illustrated in Fig. 5.

As a first example, let us consider the case of the exact sixfold orientation of a $\gamma_\chi = p6m$ projected

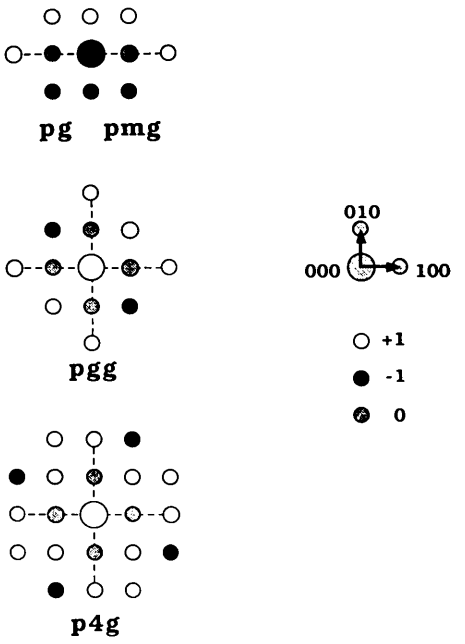

Fig. 4. Signs of the trivial symmetric linear combination of beams in the Laue orientation for the four cases of non-symmorphic 2D space groups.

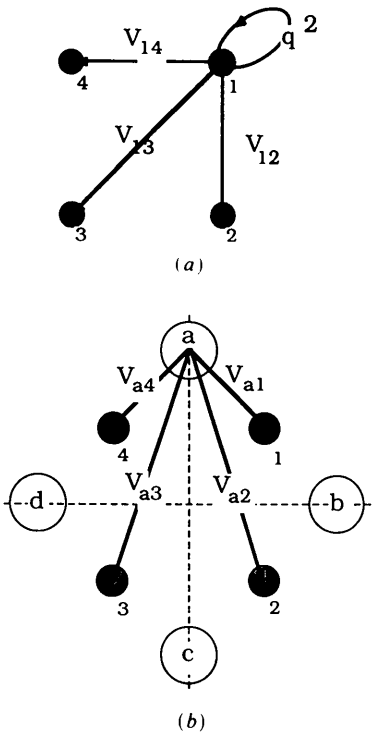

Fig. 5. (a) Diagrammatic representation of the diagonal element of the reduced Hamiltonian in the Laue symmetric case; the effective excitation error is the sum of all internal interactions between the beams of the orbit. (b) For off-diagonal elements the effective potential is the sum of the interactions of one arbitrary beam in one orbit with all the beams of the other orbit.

crystal where three **q** stars are excited (13 beams): $1=\langle 0,0\rangle$, $2=\langle 1,0\rangle$ and $3=\langle 1,1\rangle$. The totally symmetric orbits $|\mathbf{Q}\rangle$ are simply given by

$$|\mathbf{Q}_k\rangle=\frac{1}{\sqrt{6}}\sum_{i=1}^{6}|\mathbf{q}_i\rangle \tag{34}$$

for both $k=2$ and 3 orbits.

The Hamiltonian reduces to a 3×3 matrix with the matrix elements

$$\langle\chi|\mathscr{H}|\chi\rangle=0$$

$$\langle\chi|\mathscr{H}|\mathbf{Q}_2\rangle=\frac{1}{\sqrt{6}}\sum_{i=1}^{6}\langle\chi|\mathscr{H}|\mathbf{q}_i\rangle=\frac{1}{\sqrt{6}}\sum_{i=1}^{6}V_{0\mathbf{q}_i}=\sqrt{6}\,V_{10}$$

$$\langle\mathbf{Q}_2|\mathscr{H}|\mathbf{Q}_2\rangle=\frac{1}{6}\sum_{(i,j)}^{6}\langle\mathbf{q}_i|\mathscr{H}|\mathbf{q}_j\rangle=\mathbf{q}_1^2+\frac{1}{6}\sum_{(i,j,i\neq j)}^{6}V_{\mathbf{q}_i\mathbf{q}_j}$$

$$=q_1^2+2V_{10}+2V_{11}+V_{20},$$

and similarly

$$\langle\chi|\mathscr{H}|\mathbf{Q}_3\rangle=\sqrt{6}\,V_{11}$$

$$\langle\mathbf{Q}_2|\mathscr{H}|\mathbf{Q}_3\rangle=2V_{10}+2V_{20}+2V_{21}$$

$$\langle\mathbf{Q}_3|\mathscr{H}|\mathbf{Q}_3\rangle=q_2^2+2V_{11}+2V_{30}+V_{22},$$

where q is the length of one representative of the orbit and $V_{\mathbf{q}_i\mathbf{q}_j}$ are the Fourier components of the potential between the different **q** vectors of the orbit. Here, an initial 13×13 matrix has been reduced to a trivial 3×3 matrix.

As a second example, consider a $\gamma_\chi=p4g$ projected crystal with the 13 beams of the four following orbits: $1=\langle 0,0\rangle$, $2=\langle 1,1\rangle$ $3=\langle 2,0\rangle$ and $4=\langle 2,1\rangle$ (the orbit $\langle 1,0\rangle$ is dynamically absent). The restricted little group of the second orbit $\langle h,h\rangle$ is $\gamma_{\mathbf{q}_2}=cm(\mathbf{a}+\mathbf{b},\mathbf{b}-\mathbf{a})$; the coset decomposition of $p4g(\mathbf{a},\mathbf{b})$ onto $cm(\mathbf{a}+\mathbf{b},\mathbf{b}-\mathbf{a})$ is given by

$$p4g(\mathbf{a},\mathbf{b})=\{(1|0,0)+(m_x|\tfrac{1}{2},\tfrac{1}{2})+(2|0,0)+(m_y|\tfrac{1}{2},\tfrac{1}{2})\}cm(\mathbf{a}+\mathbf{b},\mathbf{b}-\mathbf{a}),$$

leading to phase coefficients all +1. The orbit $\langle 2h,0\rangle$ has little group $pg(\mathbf{a},\mathbf{b})$:

$$p4g(\mathbf{a},\mathbf{b})=\{(1|0,0)+(4|0,0)+(2|0,0)+(4^3|0,0)\}pg(\mathbf{a},\mathbf{b}),$$

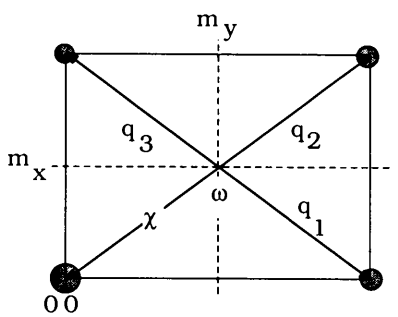

Fig. 6. Diffraction geometry of example 1.

Table 2. *Permutation table of the beams of example* 1 (*see Fig.* 6)

$p2m$	1	2	m_x	m_y
	χ	q_2	q_3	q_1
	q_1	q_3	q_2	χ
	q_2	χ	q_1	q_3
	q_3	q_1	χ	q_2
Γ	4	0	0	0

leading again to +1 phase coefficients in (32). Finally the $\langle h,k\rangle$ orbit has little group $p1(\mathbf{a},\mathbf{b})$:

$$p4g(\mathbf{a},\mathbf{b})=\{(1|0,0)+(4|0,0)+(2|0,0)+(4^3|0,0)+(m_x|\tfrac{1}{2},\tfrac{1}{2})+(m_y|\tfrac{1}{2},\tfrac{1}{2})+(m_{xy}|\tfrac{1}{2},\tfrac{1}{2})+(m_{x-y}|\tfrac{1}{2},\tfrac{1}{2})\}p1(\mathbf{a},\mathbf{b})$$

where the phase coefficients generated by the mirrors are -1.

The four basic vectors of the totally symmetric basis are, finally,

$$|\mathbf{Q}_1\rangle=|0,0\rangle;$$

$$|\mathbf{Q}_2\rangle=\tfrac{1}{2}\{|1,1\rangle+|1,-1\rangle+|-1,-1\rangle+|-1,1\rangle\};$$

$$|\mathbf{Q}_3\rangle=\tfrac{1}{2}\{|2,0\rangle+|0,2\rangle+|-2,0\rangle+|0,-2\rangle\};$$

$$|\mathbf{Q}_4\rangle=\frac{1}{2\sqrt{2}}\{|2,1\rangle-|1,2\rangle+|-1,2\rangle-|-2,1\rangle+|-2,-1\rangle-|-1,-2\rangle+|1,-2\rangle-|2,-1\rangle\}$$

from which the elements $\langle\mathbf{Q}_i|\mathscr{H}|\mathbf{Q}_j\rangle$ of the reduced 4×4 scattering matrix are easily obtained.

V.2. *Special point orientations*

There are also very interesting cases where the centre of the Ewald sphere projects at some high symmetry special points of the reciprocal lattice for which the beam reduction technique leads to remarkable results. We will illustrate these cases with three simple examples.

Example 1. 2D symmorphic $p2m$ crystal with χ at $(\frac{1}{2},\frac{1}{2})$ as shown in Fig. 6 and only the χ orbit excited. The χ star induces a 4D representation (Table 2) which can be decomposed into four irreducible 1D representations,

$$\Gamma=A_1+A_2+B_1+B_2,$$

with symmetry-adapted vectors

$$|\mathbf{Q}_1\rangle=\tfrac{1}{2}\{|\chi\rangle+|\mathbf{q}_1\rangle+|\mathbf{q}_2\rangle+|\mathbf{q}_3\rangle\}$$

$$|\mathbf{Q}_2\rangle=\tfrac{1}{2}\{|\chi\rangle+|\mathbf{q}_1\rangle-|\mathbf{q}_2\rangle-|\mathbf{q}_3\rangle\}$$

$$|\mathbf{Q}_3\rangle=\tfrac{1}{2}\{|\chi\rangle-|\mathbf{q}_1\rangle-|\mathbf{q}_2\rangle+|\mathbf{q}_3\rangle\}$$

$$|\mathbf{Q}_4\rangle=\tfrac{1}{2}\{|\chi\rangle-|\mathbf{q}_1\rangle+|\mathbf{q}_2\rangle-|\mathbf{q}_3\rangle\}.$$

Since each of these symmetry-adapted vectors belongs to a unique irreducible representation, the 4×4 Hamiltonian matrix is now diagonal with eigenvalues

$$\lambda_1 = V_{10} + V_{11} + V_{01}$$
$$\lambda_2 = V_{10} - V_{11} - V_{01}$$
$$\lambda_3 = -V_{10} - V_{11} - V_{01}$$
$$\lambda_4 = -V_{10} + V_{11} - V_{01}.$$

Here, simple symmetry considerations have directly achieved the diagonalization.

Example 2. 2D symmorphic $p3m$ projected crystal with χ at the centre of gravity of the elementary triangle (Fig. 7) with one excited orbit.

The χ orbit is again a base of representation of $3m$ (see Table 3) from which one can build the three symmetry-adapted vectors ($j = \exp 2i\pi/3$)

$$|\mathbf{Q}_1\rangle = \frac{1}{\sqrt{3}}\{|\chi\rangle + |\mathbf{q}_1\rangle + |\mathbf{q}_2\rangle\}$$
$$|\mathbf{Q}_2\rangle = \frac{1}{\sqrt{3}}\{|\chi\rangle + j|\mathbf{q}_1\rangle + j^2|\mathbf{q}_2\rangle\}$$
$$|\mathbf{Q}_3\rangle = \frac{1}{\sqrt{3}}\{|\chi\rangle + j^2|\mathbf{q}_1\rangle + j|\mathbf{q}_2\rangle\}.$$

The induced representation is the sum of a 1D and a 2D irreducible representation,

$$\Gamma = A_1 + E.$$

In the E 2D subspace spanned by $\{|\mathbf{Q}_2\rangle, |\mathbf{Q}_3\rangle\}$, it is possible to perform an additional change of basis in order to make one of the two generating vectors perpendicular to $|\chi\rangle$. Indeed, let $|\mathbf{Q}'_2\rangle$ and $|\mathbf{Q}'_3\rangle$ be the new kets of E defined by

$$|\mathbf{Q}'_2\rangle = \frac{1}{\sqrt{6}}\{2|\chi\rangle - |\mathbf{q}_1\rangle - |\mathbf{q}_2\rangle\}$$
$$|\mathbf{Q}'_3\rangle = \frac{i}{\sqrt{2}}\{|\mathbf{q}_1\rangle - |\mathbf{q}_2\rangle\}.$$

$|\mathbf{Q}'_3\rangle$ is perpendicular to $|\chi\rangle$ and can therefore be disregarded; we finally obtain the two pertinent eigenvalues of the problem by calculating the Hamiltonian diagonal matrix on the eigenbasis $\{|\mathbf{Q}_1\rangle, |\mathbf{Q}'_2\rangle\}$:

$$\lambda_1 = 2V_{10}, \qquad \lambda_2 = -V_{10}.$$

Table 3. *Permutation table of the beams of example* 2 (*see Fig.* 7)

$p3m$	1	3	3^2	m_1	m_2	m_3
	χ	q_1	q_2	q_1	q_2	χ
	q_1	q_2	χ	χ	q_1	q_2
	q_2	χ	q_1	q_2	χ	q_1
Γ	3	0	0	1	1	1

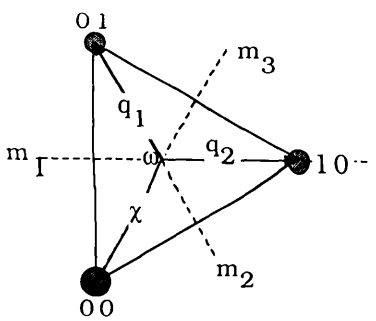

Fig. 7. Diffraction geometry of example 2.

Example 3. 2D symmorphic $p4m$ projected crystal with χ at $(\frac{1}{2}, \frac{1}{2})$ with one excited orbit (Fig. 8).

As in the previous cases, the χ orbit is a base of representation of $p4m$. From Table 4, the representation is found to be

$$\Gamma = A_1 + B_2 + E,$$

and the symmetry-adapted kets are given by

$$|\mathbf{Q}_1\rangle = \tfrac{1}{2}\{|\chi\rangle + |\mathbf{q}_1\rangle + |\mathbf{q}_2\rangle + |\mathbf{q}_3\rangle\}$$
$$|\mathbf{Q}_2\rangle = \tfrac{1}{2}\{|\chi\rangle - |\mathbf{q}_1\rangle + |\mathbf{q}_2\rangle - |\mathbf{q}_3\rangle\}$$
$$|\mathbf{Q}_3\rangle = \tfrac{1}{2}\{|\chi\rangle - |\mathbf{q}_1\rangle - |\mathbf{q}_2\rangle + |\mathbf{q}_3\rangle\}$$
$$|\mathbf{Q}_4\rangle = \tfrac{1}{2}\{|\chi\rangle + |\mathbf{q}_1\rangle - |\mathbf{q}_2\rangle - |\mathbf{q}_3\rangle\}$$

where $\{|\mathbf{Q}_3\rangle, |\mathbf{Q}_4\rangle\}$ span the 2D E representation. As in the previous example, an additional change in the E subspace defined by

$$|\mathbf{Q}'_3\rangle = \frac{1}{\sqrt{2}}\{|\mathbf{Q}_3\rangle + |\mathbf{Q}_4\rangle\} = \frac{1}{\sqrt{2}}\{|\chi\rangle - |\mathbf{q}_2\rangle\}$$
$$|\mathbf{Q}'_4\rangle = \frac{1}{\sqrt{2}}\{|\mathbf{Q}_3\rangle - |\mathbf{Q}_4\rangle\} = \frac{1}{\sqrt{2}}\{|\mathbf{q}_3\rangle - |\mathbf{q}_1\rangle\}$$

reduces the Hamiltonian matrix to three dimensions; the eigenvalues are the diagonal elements of the Hamiltonian on $|\mathbf{Q}_1\rangle$, $|\mathbf{Q}_2\rangle$ and $|\mathbf{Q}'_3\rangle$:

$$\lambda_1 = 2V_{10} + V_{11}$$
$$\lambda_2 = -2V_{10} + V_{11}$$
$$\lambda_3 = -V_{11}.$$

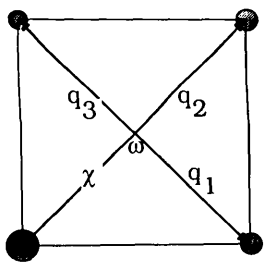

Fig. 8. Diffraction geometry of example 3.

Table 4. *Permutation table of the beams of example* 3 (*see Fig.* 8)

$p4m$	1	4^1	2	4^3	m_x	m_y	m_{xy}	$m_{x\bar{y}}$
	χ	q_1	q_2	q_3	q_3	q_1	χ	q_2
	q_1	q_2	q_3	χ	q_2	χ	q_3	q_1
	q_2	q_3	χ	q_1	q_1	q_3	q_2	χ
	q_3	χ	q_1	q_2	χ	q_2	q_1	q_3
Γ	4	0	0	0	0	0	2	2

VI. Concluding remarks

The quantum-mechanical formalism of the dynamical theory of fast-electron elastic scattering provides an elegant tool for understanding the main features of the symmetry properties of the Hamiltonian.

The basic idea of the present description is to express all symmetry operators directly in Hilbert space in order to use essentially intuitive geometric pictures for finding the symmetry-adapted basis.

As expected, the elastic Hamiltonian being real, one can always find a basis on which the scattering matrix is real. Each time a reflection is in a Bragg position, the real basis has the same size as the natural $\{|\mathbf{q}\rangle\}$ basis. The 2_1-fold dynamical extinction is an illustration of the non-trivial case $\mathcal{R}^2 = -1$ anti-unitary operation in Wigner's original work.

Applied to unitary transformations, the present technique leads to the same kind of beam reduction as developed by Takeda (1986, 1987) and is especially powerful for high-symmetry orientations. The systematic construction of the Hamiltonian matrix elements can be performed by a simple diagrammatic scheme where the self excitation (diagonal element) is replaced by a summation (with appropriate signs for non-symmorphic space groups) over all the internal coupling potentials of the beams of the orbit, and the off-diagonal elements between two different orbits are obtained by a summation of the coupling potentials between one chosen beam of the first orbit and all the beams of the second orbit.

References

BERRY, M. V. (1971). *J. Phys. C*, **4**, 697-722.

BLUME, J. (1966). *Z. Phys.* **191**, 248-253.

BUXTON, B. F., EADES, J. A., STEEDS, J. W. & RACKHAM, G. M. (1976). *Philos. Trans. R. Soc. London*, **281**, 171-194.

CORNIER, M., PORTIER, R. & GRATIAS, D. (1986). Proc. XIth Int. Congr. on Electron Microscopy, Kyoto, pp. 195-198.

COWLEY, J. M. (1975). *Diffraction Physics*. New York: North-Holland.

COWLEY, J. M. & MOODIE, A. F. (1957). *Acta Cryst.* **10**, 609-619.

EADES, J. A. (1980). *Physics of Modern Materials*, Vol. 1. Vienna: IAEA.

FISHER, P. M. (1968). *Jpn. J. Appl. Phys.* **7**, 191-199.

FUKUHARA, A. (1966). *J. Phys. Soc. Jpn*, **21**, 2645-2662.

GJØNNES, J. & MOODIE, A. F. (1965). *Acta Cryst.* **19**, 65.

GOODMAN, P. & MOODIE, A. F. (1974). *Acta Cryst.* **A30**, 280-290.

GRATIAS, D. & PORTIER, R. (1983). *Acta Cryst.* **A39**, 576-584.

HOWIE, A. & WHELAN, M. J. (1961). *Proc. R. Soc. London Ser. A*, **263**, 217-237.

KAMBE, K. (1967). *Z. Naturforsch. Teil A*, **22**, 422-431.

KOGISO, M. & TAKAHASHI, H. (1977). *J. Phys. Soc. Jpn.* **42**, 223-229.

MESSIAH, A. (1965). *Mécanique Quantique*. Paris: Dunod.

SEITZ, F. (1936). *Ann. Math. Stat.* **37**, 17-35.

STURKEY, L. (1957). *Acta Cryst.* **10**, 858-859.

STURKEY, L. (1962). *Proc. Phys. Soc. London*, **80**, 321-354.

TAKEDA, M. (1986). Proc. XIth Int. Congr. on Electron Microscopy, Kyoto, pp. 749-751.

TAKEDA, M. (1987). *Phys. Status Solidi A*, **101**, 25-36.

TINNAPPEL, A. & KAMBE, K. (1975). *Acta Cryst.* **A31**, S6.

TOURNARIE, M. (1960). *Bull. Soc. Fr. Minéral. Cristallogr.* **83**, 179-186.

VAN DYCK, D. (1980). *J. Microsc.* **119**, 141-152.

VERGASOV, V. L., CHUKHOBSKII, F. N. & PINSKER, Z. G. (1982). *Kristallografiya*, **27**, 446-456.

WIGNER, E. P. (1932). *Göttinger Nachr.* **31**, 546-559.

Acta Cryst. (1988). **A44**, 798-805

Imaging Tunnel Atoms in Intergrowth Tungsten Bronzes

BY LARS KIHLBORG AND MARGARETA SUNDBERG

Department of Inorganic Chemistry, Arrhenius Laboratory, University of Stockholm, S-10691 Stockholm, Sweden

(*Received* 5 *January* 1988; *accepted* 6 *April* 1988)

Abstract

Crystals of caesium and rubidium intergrowth tungsten bronze (ITB) have been studied by high-resolution electron microscopy. The structure of these consists of slabs of WO_3 type, intergrown with slabs of hexagonal tungsten bronze (HTB) type containing hexagonal tunnels in which the alkali atoms are accommodated. In the images of thicker parts the hexagonal tunnels are clearly revealed. In the thin parts the HTB structure mostly appears as a hexagonal pattern of dots of equal intensity and the tunnels are not recognizable. This applies particularly to Cs ITB but also in many instances to Rb ITB. Image simulations, assuming known or estimated degrees of filling of the tunnels with alkali, show a clear difference in contrast at the tungsten and alkali positions, especially at certain focus settings. The dis-

0108-7673/88/060798-08$03.00